# DYNAMIC SOURCE LOCALIZATION AND FUNCTIONAL CONNECTIVITY ESTIMATION WITH STATE-SPACE MODELS: PRELIMINARY FEASIBILITY ANALYSIS

*Jose M. Sanchez-Bornot*[1], *Roberto C. Sotero*[2], *Damien Coyle*[1,3]

[1] Intelligent Systems Research Centre, School of Computing, Engineering and Intelligent Systems, Ulster University, Magee campus, Derry~Londonderry, BT48 7JL, UK.
[2] Department of Radiology and Hotchkiss Brain Institute, University of Calgary, Calgary, AB, Canada.
[3] The Bath Institute for the Augmented Human, University of Bath, Bath, BA2 7AY, UK.

## ABSTRACT

Dynamic imaging of source and functional connectivity (FC) using electroencephalographic (EEG) signals is essential for understanding the brain and cognition with sufficiently affordable technology to be widely applicable for studying changes associated with healthy ageing and the progression of neuropathology. We present an application for group analysis of recently developed state-space models and algorithms for simultaneously estimating the large-scale EEG inverse and FC problems. This approach reduces estimation bias and facilitates a detailed exploration and investigation of neuronal dynamics compared to current techniques. We present feasibility analyses for simulated and real EEG event-related data. The latter analysis uses a sixteen subjects EEG (Wakeman and Henson's) database, with signals recorded during a face-processing task. We implement a state-space methodology efficiently using an alternating least squares (ALS) algorithm. This application to neuroimaging analysis may be critical to reliably capture the brain dynamics despite interindividual variability, as demonstrated by the results presented.

***Index Terms***— State-space models, EEG/MEG event-related source imaging, Dynamic functional connectivity, Feasibility analysis, Machine learning

## 1. INTRODUCTION

Dynamic source imaging and functional connectivity (FC) analyses are essential to unravel the timing and localization of cognitive processing and identify the underlying brain integration and segregation networks [1]. The use of magneto/electro-encephalography (MEG/EEG) techniques is essential to study these problems due to their high-temporal resolution and non-invasiveness. Remarkably, the low cost and portability of wearable neurotechnology/EEG make it ideal for supporting the broader application of neuroimaging methods that may lead to a better understanding of brain dynamics.

The current scientific efforts to extend the application of neuroimaging methods are seriously undermined by the amount of different source localization and functional connectivity methods, which regularly produce diverging results. At the same time, community experts have differing views on the importance of the same methods and their validation, with contradictory results and still inconclusive reproducibility analyses [2, 3].

Amidst recent examples, Hincapie et al. [4] showed that hyperparameter values selected for optimization of source power estimation differed significantly from selected values that optimize coherence-based FC assessment. The same researchers also evaluated the combination of multiple source localization and FC methods with a Monte-Carlo simulation without obtaining a clear advantage of any pipeline in the simulated scenarios [5]. Mahjoory et al. [2] also compared different pipelines through a general reproducibility analysis, which implemented combinations of inverse solutions and FC methods while using the implementation provided in three different software. Also, they included different methods to solve the EEG forward problem. The main findings were that reproducibility is higher when using spectral methods, particularly with sensor-based instead of source solutions, and lower when using undirected FC, but still significantly higher than the reproducibility of results in directed FC analysis.

In summary, the main concerns from these studies are that the main results show that source methods do not significantly improve their sensor-based counterparts and that most methods employed have issues with volume conduction. The latter also manifests in the source solutions due to the ill-conditioned and non-uniqueness of inverse methods and the mixing of sensor signals.

On the other hand, there is an increasing agreement that state-space models can unify the different approaches and produce less biased results [6, 7, 8, 9]. Recent studies have demonstrated that two-step approaches, i.e., approaches that first estimate the source time series from which the FC measures are calculated, such as those mentioned above, can lead to suboptimal/biased solutions [7, 10].

Our study also supports the hypothesis that state-space models can naturally model the mutual dependence between these solutions and may produce better results than alternative two-step methods [7, 10, 11]. Primarily, we

demonstrate the feasibility of our recently proposed methodology [11] for group statistical analysis.

## 2. RELATED WORK

In a recent investigation by our group [11], we introduced the state-space models and estimation algorithms applied in the present study. Similarly, state-space models have also been used to solve brain source localization and functional connectivity problems simultaneously. Long et al. [6] claimed, as we do, to solve these models in high dimensions and use high-performance computing. However, most related works use assumptions to simplify the calculations, which may lead to bias [6, 9]. In contrast, our methodology does not utilize any simplification tricks. Other researchers have also used a similar trick to ours to establish the connection between source localization and FC estimators, which statistically constrain each other, as observed with mathematical closed-form solutions [11]. Although they could have exploited this relationship algorithmically, they used Bayesian filtering to estimate the solutions [10]. Finally, Manomaisaowapak et al. [12] also proposed a similar approach to ours while considering a group LASSO penalty for producing sparse estimators. However, their study used priori-selected regions to reduce dimensionality, which we avoid in our proposed methodology.

## 3. STATE-SPACE MODELS OF BRAIN DYNAMICS

We estimate the dynamic source imaging and FC problems using state-space models with an approach similar to the sliding-window technique [13]. In particular, we state the state-space model as follows:

$$\mathbf{y}_t = \mathbf{B}\mathbf{x}_t + \mathbf{w}_t; \text{ for } t = 1,2,\dots,T, \quad (1)$$

$$\mathbf{x}_t = \sum_{p=1}^{P} \mathbf{A}_p \mathbf{x}_{t-p} + \mathbf{v}_t; \text{ for } t = P+1,\dots,T, \quad (2)$$

where $\mathbf{y}_t$ and $\mathbf{x}_t$ represent the observation and state dynamics, respectively. $\mathbf{B} \epsilon \mathcal{R}^{M\times N}$ is the lead field matrix, and $\mathbf{A}_p \in \mathcal{R}^{N\times N}$, $p = 1,\dots,P$, are the autoregressive matrices, enabling the linear modelling of neuronal dynamics. The noise terms, $\mathbf{v}_t \epsilon \mathcal{R}^{N\times 1} \sim N(0, \sigma_s^2 \mathbf{I}_N)$ and $\mathbf{w}_t \epsilon \mathcal{R}^{M\times 1} \sim N(0, \sigma_o^2 \mathbf{I}_M)$, are identically and independently distributed (i.i.d.) Gaussian processes, which represent uncontrolled perturbations.

Here, we use a more general framework to estimate state-space models, as presented for the analysis of event-related potential (ERP) activity, using the optimization problem:

$$F = \frac{1}{TE}\sum_{e=1}^{E}\left(\sum_{t=1}^{T}\left\|\mathbf{y}_t^{(e)} - \mathbf{B}\mathbf{x}_t^{(e)}\right\|_2^2 + \lambda\sum_{t=P+1}^{T}\left\|\mathbf{x}_t^{(e)} - \sum_{p=1}^{P}\mathbf{A}_p\mathbf{x}_{t-p}^{(e)}\right\|_2^2 + \lambda\sum_{t=1}^{P}\left\|\mathbf{x}_t^{(e)}\right\|_2^2\right) + \lambda_2\|\mathbf{A}\|_F^2, \quad (3)$$

$$\hat{\mathbf{x}}, \hat{\mathbf{A}} = \underset{\mathbf{x},\mathbf{A}}{argmin}\, F(\mathbf{x}, \mathbf{y}, \mathbf{A}, \mathbf{B}, \lambda, \lambda_2), \quad (4)$$

where $\mathbf{y}_t^{(e)}$ and $\mathbf{x}_t^{(e)}$ represent the measured and estimated dynamics for epochs $e = 1,\dots,E$. Here, $\mathbf{y}$ and $\mathbf{x}$ represent the dynamics for all epochs, i.e., $\mathbf{y} = \left\{\mathbf{y}_t^{(e)}\right\}_{t=1,\dots,T}^{e=1,\dots,E}$, and similarly $\mathbf{A} = \{\mathbf{A}_p\}_{p=1,\dots,P}$. Details for implementing this regularization framework for state-space models, which includes the data-driven estimation of the model hyperparameters (i.e., $\lambda$ and $\lambda_2$), are provided in [11].

## 4. EXPERIMENTAL SETTINGS

We demonstrate the state-space models' framework with simulated and real EEG data used for feasibility analyses to validate the application for group statistical analysis. Details of the simulations and EEG dataset are provided below.

### 4.1. Simulated data

We simulated thirteen subjects where each subject's lead field matrix was generated by (1) using the Gaussian normal distribution and (2) normalizing the lead fields per column a posteriori. Time series corresponding to five interacting regions were generated using an autoregressive model with order $P = 5$. We controlled the signal-to-noise ratio by fixing the state noise standard deviation as $\sigma_s = 1$ while testing different observation noise scales by setting $\sigma_s = 0.1$ and $\sigma_s = 0.5$. Lastly, we generated random autoregressive matrices for each subject using a Gaussian distribution with mean at the entries of a population connectivity matrix, which is:

$$\mathbf{A} = \left\{ \begin{bmatrix} 0.8 & 0 & 0 & 0 & 0 \\ 0 & 0.8 & 0 & 0 & 0 \\ 0 & 0 & 0.8 & 0 & 0 \\ 0 & 0 & 0 & 0.8 & 0 \\ 0 & 0 & 0 & 0 & 0.8 \end{bmatrix}, -\begin{bmatrix} 0.5 & 0 & 0 & 0 & 0 \\ 0 & 0.5 & 0 & 0 & 0 \\ 0 & 0 & 0.5 & 0 & 0 \\ 0 & 0 & 0 & 0.5 & 0 \\ 0 & 0 & 0 & 0 & 0.5 \end{bmatrix}, \right.$$

$$\left. \begin{bmatrix} 0 & 0 & 0 & 0 & 0 \\ 0.3 & 0 & 0 & 0 & 0 \\ 0 & 0 & 0 & 0 & 0 \\ 0 & 0 & 0 & 0 & 0 \\ 0 & 0 & 0 & 0 & 0 \end{bmatrix}, \begin{bmatrix} 0 & 0 & 0 & 0 & 0 \\ 0 & 0 & 0 & 0 & 0 \\ 0.3 & 0 & 0 & 0 & 0 \\ 0 & 0 & 0 & 0 & -0.3 \\ 0 & 0 & 0 & 0.3 & 0 \end{bmatrix}, \begin{bmatrix} 0 & \cdots & 0 \\ 0 & \cdots & 0 \\ 0 & \cdots & 0 \\ 0 & \cdots & 0 \\ 0 & \cdots & 0 \end{bmatrix} \right\}.$$

where only the intraregional connections were perturbed, i.e., $A_{i,i,p}^{(s)} \sim N(A_{i,i,p}, \sigma_{conn}^2)$, for $i = 1,\dots,5$, $p = 1,2$, and $s = 1,\dots,13$, where we set $\sigma_{conn} = 0.1$ in order to minimize the instability of the simulated time series. For all the synthetic connectivity matrices, the stability of each multivariate autoregressive VAR(P) model was checked theoretically by reducing it to the corresponding VAR(1) general form and guaranteeing that the eigenvalues of the latter matrix are in the unit radius complex circle [14]. We also checked it numerically using a threshold for controlling larger values after generating 10,000 samples for 200 epochs, finally retaining only the last $T = 25$ or $T = 125$ samples for two different simulated scenarios.

As an illustration, for two simulated subjects, the first autoregressive diagonal matrices ($p = 1,2$) are:

$$\mathbf{A}_{p=1,2}^{(Subject\ \#1)} = \left\{ \begin{matrix} diag([0.85,0.98,0.57,0.89,0.83]), \\ -diag([0.63,0.54,0.47,0.14,0.22]) \end{matrix} \right\},$$

$$\mathbf{A}_{p=1,2}^{(Subject\ \#2)} = \left\{ \begin{matrix} diag([0.85,0.87,0.68,0.71,0.77]), \\ -diag([0.55,0.37,0.38,0.65,0.23]) \end{matrix} \right\}.$$

Fig. 1 shows a graphical representation and colormap for the simulated ground-truth matrices (top rows), as well as the plot for the power spectral density (PSD) measure calculated from the synthetic time series generated for the two simulated subjects above (bottom row). PSD curves are calculated assuming the sampling frequency $F_s = 125$ Hz. In this simulated example, note that the small random perturbations to the diagonal entries, as described above, are sufficient to create a rich variation of the spectrum peak in the range from Theta (4-7.5 Hz) to Beta (13-30 Hz) brain rhythms.

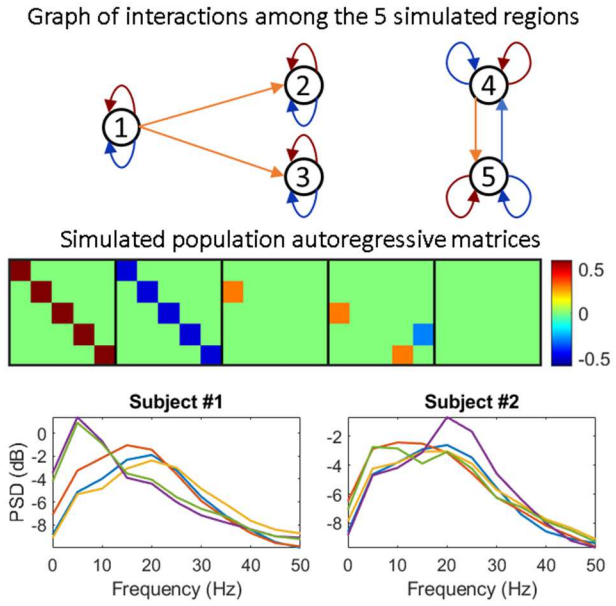


**Fig. 1:** Graph and colormap of interactions among the ground-truth 5 simulated regions, together with examples of the power spectral density (PSD) for two simulated subjects, where the latter is calculated from the state-space model latent (variables) time series generated with the autoregressive matrices shown in the main text.

### 4.2. Preprocessing of real EEG event-related data

For the EEG event-related data analysis, we used the data and custom Matlab scripts provided in the Wakeman and Henson study [15]. From 70 original EEG channels, some were rejected for each subject following information provided in the scripts. Posteriorly, the signals were preprocessed using a low-pass 25 Hz Butterworth filter with order five and downsampled to $F_s = 125$ Hz. EEG signals were re-referenced using the average reference, and epochs were extracted for the time window [-300; 1000] ms for the famous face stimulus. Then, epoch signals were baseline corrected using the pre-stimulus time window [-300; -100] ms. We rejected epochs with corresponding electrooculogram (EOG) signals higher than 100 μV to control for eye movements, resulting in more than 200 remaining epochs per subject on average. Finally, we used the Fieldtrip toolbox [16] to calculate the EEG lead field using a boundary element method with three compartments and tissue conductivities defined by default in the toolbox settings. The last procedure used the MRI images and skin/skull/cortical surface mesh data, provided together with the EEG channel locations.

## 5. RESULTS

### 5.1. Analysis of synthetic data

Fig. 2 shows the estimated autoregressive coefficients for a particular simulated subject (top row). The matrices are arranged from left to right for each lag $p = 1, \dots, 5$. As can be appreciated, this estimator approximates the ground-truth connectivity with reasonable accuracy, as highlighted by the corresponding pruned outcome (bottom row), in which the one sample Student's test allowed the evaluation of significant nonzero connections, with the degree of freedom $N_s - 1$, with $N_s = 13$ denoting the number of subjects in the simulated dataset. Particularly, note that the missed estimated diagonal entries for the negative connections (i.e., lagged influences for $p = 2$) are those related to the smaller entries of the simulated matrix $\mathbf{A}_{p=2}^{(Subject\ \#1)}$, as shown in Section 4.1.

In the analysis, the use of Bonferroni's correction controls for multiple comparisons, where the standard $p$-value (0.05) is divided by the number of statistical tests ($N^2P = 125$) to produce the statistical cutoff value ($4 \times 10^{-4}$).

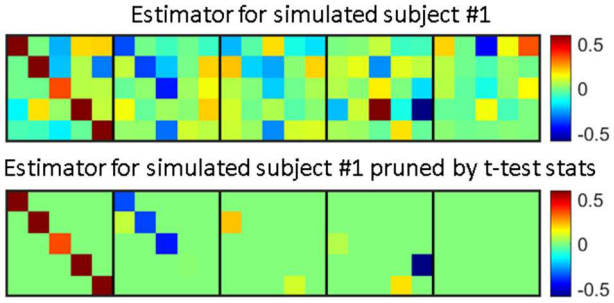


**Fig. 2:** Estimated autoregressive coefficients for one simulated subject (top row) with its pruned outcome after using the one-sample Student's test for the whole simulated population (bottom row).

Moreover, Fig. 3 shows the grand mean average of the estimated autoregressive matrices calculated from all the simulated subjects and pruned using the Student's test statistics, separately for each of the four different simulated scenarios: (1) with a smaller or larger number of samples, and (2) with a smaller or larger observation noise. By simple visual inspection as compared to Fig. 1 (middle row), the results show a very high rate of true positive findings with very few false positive errors. These results demonstrate that our regularization framework for estimating state-space models can produce excellent results for group statistical analysis. This methodology is evaluated next with real data.

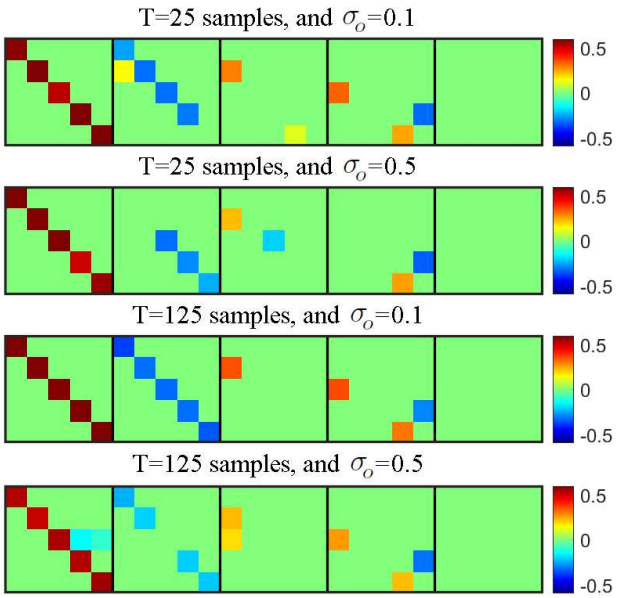


**Fig. 3:** Grand mean average of estimated autoregressive coefficients for the different simulated scenarios.

### 5.2. Analysis of real EEG event-related data

Three subjects had to be discarded from sixteen subjects in the Wakeman and Henson dataset [15] due to numerical issues with Fieldtrip for the lead field calculation. After reducing the provided cortical meshes of 8196 points to 2052 dipole locations, another two subjects were discarded due to the rough correspondence of dipoles to the template dipoles in the reduced parcellation.

Fig. 4 shows a sparse plot (Matlab function "spy") for the significant connections selected using the one-sample Student's test as above, but showing only the connections with $p$-values lower than $10^{-4}$, highlighted separately with different colors for the positive and negative coefficients, as well as using a higher-size point marker for the more significant findings. Notably, for lag 1, autoconnections are mainly positive and to a lesser degree, for lag 3, autoconnections are mainly negative. In this analysis, we considered three overlapped time windows to explore the FC dynamical changes: approximately 100 to 200, 150 to 250, and 200 to 300 milliseconds.

Additionally, we calculated the ERPs from the source time series, which were estimated together with the autoregressive matrices. As illustration, Fig. 5 shows the source activations for a single subject for the peak of maximum activity of the ERP components in different time windows, revealing the activation of the visual ventral stream as anticipated for the brain processing of face information. Note that sources are moderately symmetrical with greater magnitude in the inferotemporal than in occipital regions (0.15 vs 0.10) at 164 ms (see colormap). In contrast, at 276 ms, inferotemporal regions' activity is decreased. Also, note the lower but still prominent activity in the frontal lobe.

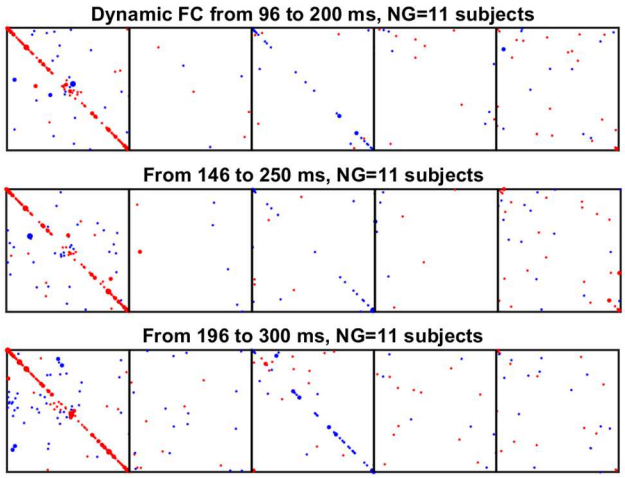


**Fig. 4:** Significant connections among the 2052 cortical dipoles sampled from the SMP12 medium-size cortex template. Lagged connections are shown along the columns for $p = 1, \ldots, 5$. Red/blue colors denote positive/negative influences. The larger, middle or smaller size markers correspond to very highly significant ($p < 10^{-6}$), highly significant ($10^{-6} \leq p < 10^{-5}$), and significant ($10^{-5} \leq p < 10^{-4}$) connections.

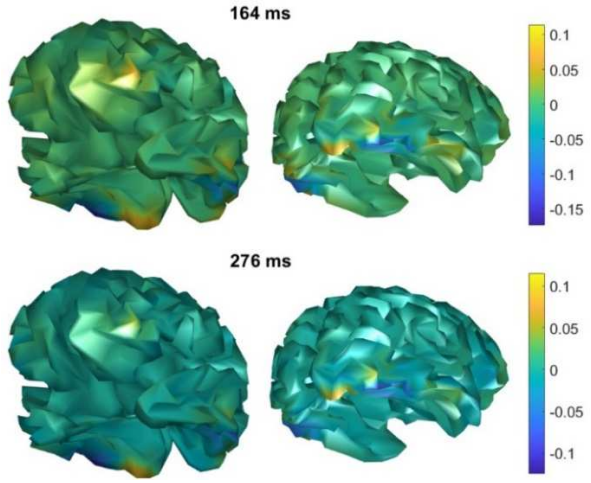


**Fig. 5:** Source ERP activity peaks for face information processing during the 1st and 3rd time windows. Left: frontotemporal view (left hemisphere). Right: occipitotemporal view (right hemisphere).

## 6. CONCLUSION

Despite the small number of samples in our study, we have demonstrated the feasibility of using our proposed state-space models' framework [11] for group statistical analysis using simulated and real EEG data analyses. In future studies, we plan to further validate this methodology with larger datasets for different experimental conditions. The main challenges are (1) the computational cost, as analyzing one subject can take few days and uses about 0.5 terabytes of RAM for a 17-core parallel job, and (2) methodologically, as we plan to increase the number of brain cortical/volume dipoles, which overall will increase the demand on resources.

## 7. REFERENCES


[1] F. Lopes da Silva, "EEG and MEG: Relevance to Neuroscience," *Neuron*, vol. 80, no. 5, pp. 1112–1128, Dec. 2013, doi: 10.1016/j.neuron.2013.10.017.

[2] K. Mahjoory, V. V. Nikulin, L. Botrel, K. Linkenkaer-Hansen, M. M. Fato, and S. Haufe, "Consistency of EEG source localization and connectivity estimates," *Neuroimage*, vol. 152, pp. 590–601, 2017, doi: 10.1016/j.neuroimage.2017.02.076.

[3] C. T. Briels, D. N. Schoonhoven, C. J. Stam, H. de Waal, P. Scheltens, and A. A. Gouw, "Reproducibility of EEG functional connectivity in Alzheimer's disease," *Alzheimers. Res. Ther.*, vol. 12, no. 1, p. 68, Dec. 2020, doi: 10.1186/s13195-020-00632-3.

[4] A. S. Hincapié *et al.*, "MEG connectivity and power detections with minimum norm estimates require different regularization parameters," *Comput. Intell. Neurosci.*, vol. 2016, pp. 12–18, 2016, doi: 10.1155/2016/3979547.

[5] A. S. Hincapié *et al.*, "The impact of MEG source reconstruction method on source-space connectivity estimation: A comparison between minimum-norm solution and beamforming," *Neuroimage*, vol. 156, no. August 2016, pp. 29–42, 2017, doi: 10.1016/j.neuroimage.2017.04.038.

[6] C. J. Long, P. L. Purdon, S. Temereanca, N. U. Desai, M. S. Hämäläinen, and E. N. Brown, "State-space solutions to the dynamic magnetoencephalography inverse problem using high performance computing," *Ann. Appl. Stat.*, vol. 5, no. 2 B, pp. 1207–1228, 2011, doi: 10.1214/11-AOAS483.

[7] F. Van de Steen, L. Faes, E. Karahan, J. Songsiri, P. A. Valdes-Sosa, and D. Marinazzo, "Critical Comments on EEG Sensor Space Dynamical Connectivity Analysis," *Brain Topogr.*, vol. 32, no. 4, pp. 643–654, Jul. 2019, doi: 10.1007/s10548-016-0538-7.

[8] K. J. Friston, L. Harrison, and W. Penny, "Dynamic causal modelling," *Neuroimage*, vol. 19, no. 4, pp. 1273–1302, 2003, doi: 10.1016/S1053-8119(03)00202-7.

[9] A. Galka, O. Yamashita, T. Ozaki, R. Biscay, and P. Valdés-Sosa, "A solution to the dynamical inverse problem of EEG generation using spatiotemporal Kalman filtering," *Neuroimage*, vol. 23, no. 2, pp. 435–453, 2004, doi: 10.1016/j.neuroimage.2004.02.022.

[10] S. N. Puthanmadam, F. Tronarp, S. Särkkä, and L. Parkkonen, "Joint estimation of neural sources and their functional connections from MEG data," *Preprint*, pp. 1–24, 2020, doi: 10.1101/2020.10.04.325563.

[11] J. M. Sanchez-Bornot, R. C. Sotero, S. Kelso, and D. Coyle, "Solving large-scale MEG/EEG source localization and functional connectivity problems simultaneously using state-space models," *arXiv Prepr.*, Aug. 2022, [Online]. Available: http://arxiv.org/abs/2208.12854.

[12] P. Manomaisaowapak, A. Nartkulpat, and J. Songsiri, "Granger Causality Inference in EEG Source Connectivity Analysis: A State-Space Approach," *IEEE Trans. Neural Networks Learn. Syst.*, pp. 1–11, 2021, doi: 10.1109/TNNLS.2021.3096642.

[13] R. Hindriks *et al.*, "Can sliding-window correlations reveal dynamic functional connectivity in resting-state fMRI?," *Neuroimage*, vol. 127, pp. 242–256, 2016, doi: 10.1016/j.neuroimage.2015.11.055.

[14] H. Lütkepohl, *Introduction to multiple time series analysis*. Springer Science & Business Media, 2013.

[15] D. G. Wakeman and R. N. Henson, "A multi-subject, multi-modal human neuroimaging dataset," *Sci. data*, vol. 2, p. 150001, 2015, doi: 10.1038/sdata.2015.1.

[16] R. Oostenveld, P. Fries, E. Maris, and J. M. Schoffelen, "FieldTrip: Open source software for advanced analysis of MEG, EEG, and invasive electrophysiological data," *Comput. Intell. Neurosci.*, vol. 2011, 2011, doi: 10.1155/2011/156869.